Environmentally friendly synthesis methods to obtain the misfit $[Ca_2CoO_{3-\delta}]_{0.62}[CoO_2]$ thermoelectric material

Aline A. Emerenciano[a,1], Allan J. M. Araújo[a,1], João P. F. Grilo[b], Daniel A. Macedo[c,*]
Shahed Rasekh[b], Andrei V. Kovalevsky[b], Carlos A. Paskocimas[a], Rubens M. Nascimento[a]

[a] Materials Science and Engineering Postgraduate Program, UFRN, 59078-970 Natal, Brazil

[b] CICECO – Aveiro Institute of Materials, Department of Materials and Ceramic Engineering, University of Aveiro, 3810-193 Aveiro, Portugal

[c] Materials Science and Engineering Postgraduate Program, UFPB, 58051-900 João Pessoa, Brazil

Abstract

This work reports the microstructural and thermoelectric characterization of the misfit $[Ca_2CoO_{3-\delta}]_{0.62}[CoO_2]$ compound obtained by a solid-state synthesis using mollusk shells and a proteic sol-gel method, which uses gelatin as a polymerizing agent. The results clearly demonstrate the capability of these routes to produce pure $Ca_3Co_4O_9$ with plate-like morphology. Sintered ceramic samples show randomly oriented grains and relative densities in the range of 63-67%. The obtained microstructures provide reasonable electrical properties and result in competitive thermoelectric performance for the material prepared by the proteic sol-gel synthesis (P.F. of 205 $\mu W/K^2$ m at 700 ºC).

Keywords: $Ca_3Co_4O_9$; Ceramics; Environmentally friendly precursors; Proteic sol-gel synthesis; Electrical properties.

*Corresponding author: damaced@pq.cnpq.br (Daniel A. Macedo). Tel.: +55 83 32167860; fax: +55 83 32167906.

[1]These authors contributed equally to this work.

1. Introduction

Thermoelectric (TE) materials have a high potential for energy recovery from waste heat energy produced from power generation processes [1]. In this context, $[Ca_2CoO_{3-\delta}]_{0.62}[CoO_2]$ with a misfit layered structure, also known as $Ca_3Co_4O_9$ (C349), has received special attention as a promising *p*-type TE material, simultaneously possessing a high power factor, low thermal conductivity, remarkable thermal and chemical stability at high temperatures, and relatively low associated costs [2–8]. Several synthesis techniques to obtain C349 have been investigated: conventional solid-state reaction method [9–12], sol-gel [6,13,14], co-precipitation [15], molten salt method [16], citrate method [17–19], among others. These synthesis routes are followed by heat-treatment steps that may negatively affect the phase stability, stoichiometry and composition [8], while also resulting in excessive grain growth. Our research group have successfully prepared C349 by novel environmentally friendly methods [20,21] and further investigated their electrochemical performance as Solid Oxide Fuel Cell (SOFC) cathode materials. These methods involved the use of mollusk shell powder in a solid-state reaction [20] and commercial gelatin in a proteic sol-gel method [21]. In this paper, these two synthesis procedures are for the first time used as alternative processing routes for the preparation of C349-based thermoelectrics. Relevant microstructural and electrical transport properties of C349 synthesized by a well-known citrate method (for the sake of comparison) is also discussed.

2. Experimental

Three synthesis methods were used: solid-state reaction in the conditions of high energy milling (C349-M), proteic sol-gel (C349-G) and citrate synthesis (C349-C). For the C349-M, the precursor powder was synthesized by using mollusk shell powder and Co_3O_4, as reported elsewhere [22]. These materials were mixed/milled in an alcohol-based suspension at 400 rpm for 10 h, dried at 110 °C for 12 h and granulated through a 200-mesh sieve. In the case of C349-G, the sample was fabricated as previously reported in [21]. Details on the synthesis of calcium cobaltite by the citrate method (C349-C) can be found in Supplementary data. The obtained three precursor powders were further calcined at 900 °C for 2 h, pressed at 200 MPa and sintered at 900°C for 24 h using a heating rate of 3 °C min^{-1}. Details on the characterization of powders and sintered samples can be found in Supplementary data.

3. Results and discussion

Fig. 1 shows XRD patterns and STEM images of the powders. No discernible change was observed in the XRD patterns when the dwell time was raised from 2 h to 24 h (Fig. 1a-b). C349-G and C349-M showed monophasic powders consisting of the expected Ca_2CoO_3 (ICSD 151437) and CoO_2 (ICSD 151436) subsystems or, more commonly, $Ca_3Co_4O_9$. On the other hand, C349-C sample also contains $Ca_3Co_2O_6$ (C326) (ICSD 246281), as can also be seen in Fig. S1 and Table S1. The morphological characterization (Fig. 1c-d) of samples calcined at 900 °C for 2 h shows that powders prepared by the two eco-friendly synthesis methods (C349-M and C349-G) have plate-like particles. Moreover, higher agglomeration is observed in the solid-state reaction compared to the proteic sol-gel method. According to Zhang et al. [23], this fact can be explained by the formation of a polymeric resin, which contributes to the dispersion of particles. An irregularity in the morphology of C349-M particles is ascribed to the milling process.

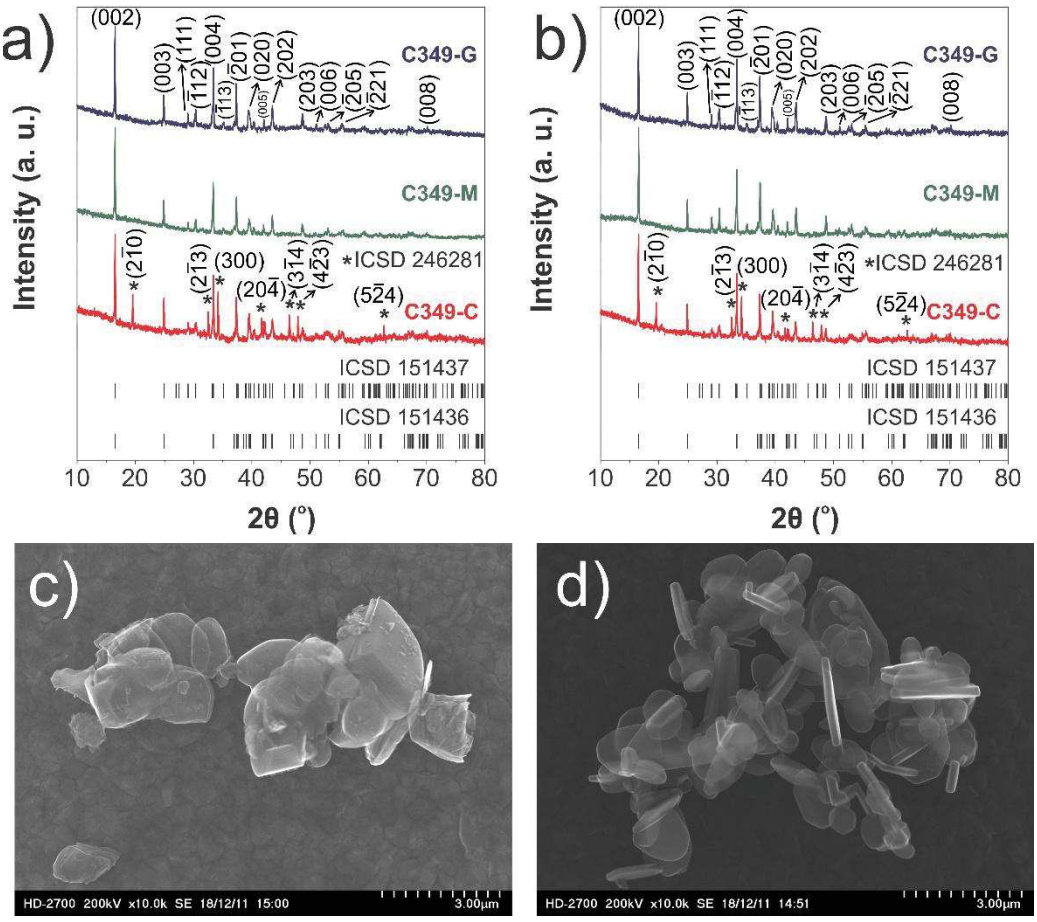

Fig. 1. Room-temperature XRD patterns of the powders heat-treated at 900 ºC for (a) 2 h and (b) 24 h. STEM of the powders calcined for 2 h: (c) C349-M and (d) C349-G.

Fig. 2 shows SEM images and EDS elemental maps of sintered pellets. It can be clearly seen that the microstructure of the C349-C (Fig. 2c) sample exhibits grains of smaller size than those of other samples (Fig. 2a and 2b). Nevertheless, all microstructures show reported typical trend of randomly oriented grains [11,24]. Relative densities of C349 pellets showed 63-67% (Table S2), in accordance with the literature [2]. Such low densities are caused by a large number of pores, which may impair the thermoelectrical properties [25,26]. Madre et al. [4] have reported that this low density is due to the maximum stability temperature of the $Ca_3Co_4O_9$ phase (926 ºC), below the eutectic point (1350 ºC), which hinders the densification process. EDS mapping (Fig. 2d-f) shows a nearly homogeneous distribution of Ca and Co elements in all sintered samples.

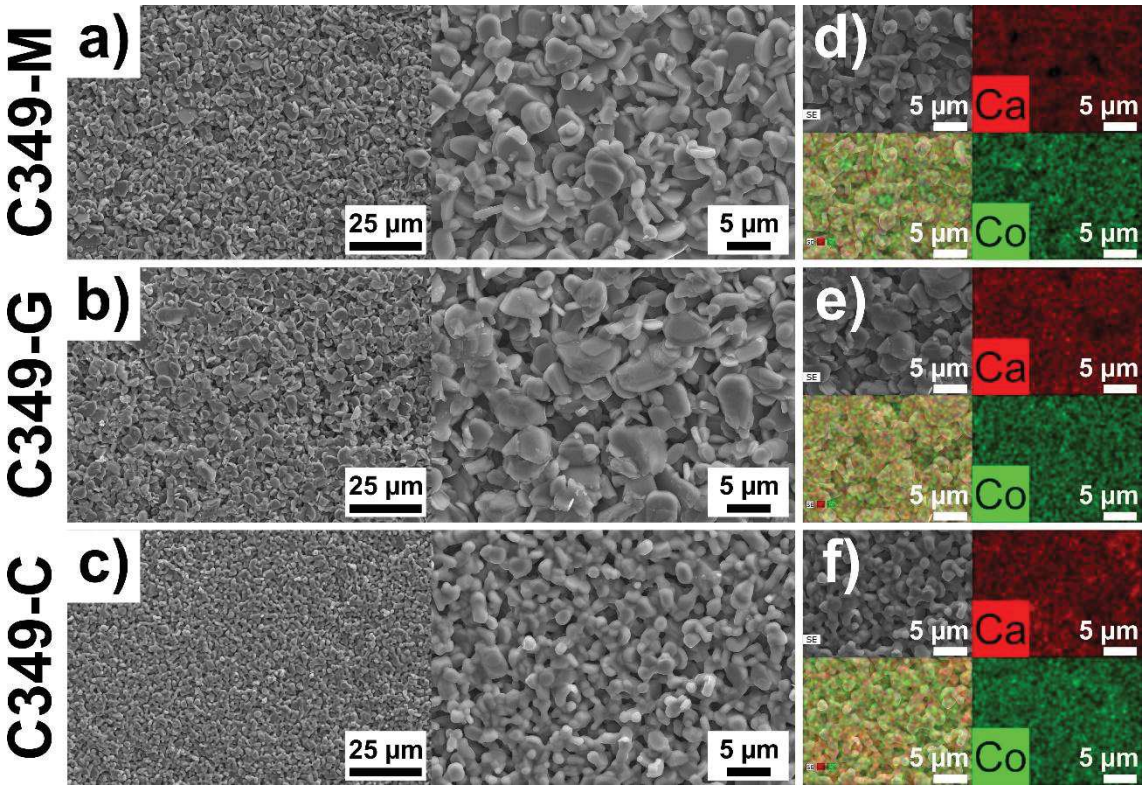

Fig. 2. SEM (a-c) and EDS (d-f) of the pellets.

Fig. 3 displays the temperature dependence of Seebeck coefficient (S), electrical resistivity (ρ) and power factor (P.F.) for all the samples. Positive values of Seebeck coefficients indicate a *p*-type semiconductor behavior. The values are quite similar for all the samples, with slightly higher S at 600-700 ºC observed for C349-C. This is in agreement with a known fact that the Seebeck coefficient is mainly determined by the band structure, and normally is not affected by the microstructural features. The

similarity of those values also confirms that the cobalt oxidation states in the sintered ceramics are controlled by the sintering procedure rather than by the differences in powder synthesis routes. On the other hand, the electrical resistivity is quite distinct along the entire temperature range, reflecting some tendencies in the microstructural evolution. C349-G sample shows semiconductor-like behavior ($d\rho/dT < 0$) between 250-550 °C and pseudometallic behavior ($d\rho/dT > 0$) above 550 °C. C349-M shows a similar behavior with a transition point at ~ 600 °C. On the contrary, C349-C shows only semiconductor-like behavior in the entire measured temperature with highest resistivity values. The C349-G sample has the lowest resistivities, followed by C349-M and C349-C. The highest values of ρ found for C349-C may be partially associated with the secondary phase C326, which possesses a low electrical conductivity [27,28]. This observation is in agreement with SEM micrographs (Fig. 2a-c), where C349-C shows the smallest grain size (Fig. 2c), with expected higher contribution of the more resistive grain boundaries to the electronic transport. Therefore, C349-G exhibits the largest P.F. values in the studied temperature range, due to possessing the lowest resistivity of all the samples.

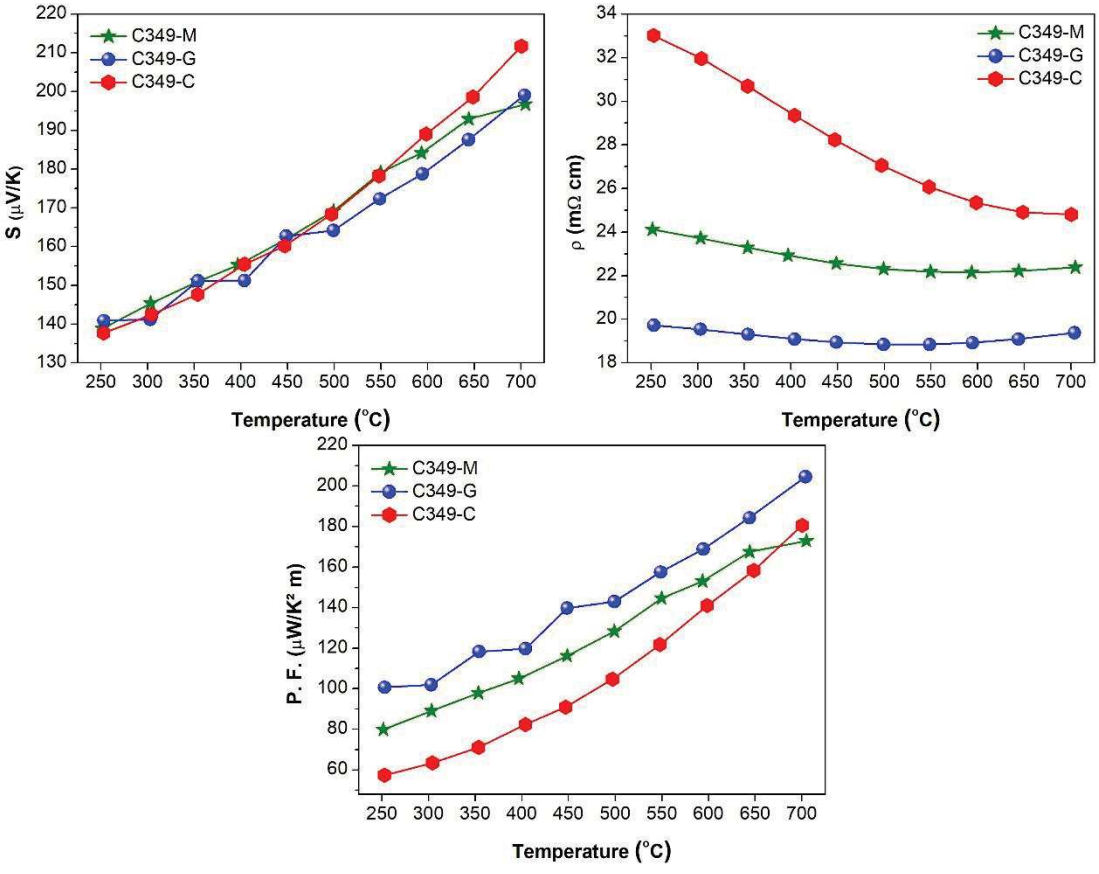

Fig. 3. Temperature dependence of the thermoelectric properties, S: Seebeck Coefficent, ρ: Electrical resistivity, and P.F.: calculated power factor.

Selected thermoelectric properties of C349 samples are listed in Table S3 and compared with the literature data for materials synthesized by other routes and processed under similar conditions. Competitive thermoelectric performance is observed for C349-G and C349-M ceramics, synthesized by environmentally friendly methods, with superior performance obtained for the C349-M. These results indicate that the proposed eco-friendly synthesis routes result in pure C349 phase and high-quality powders for obtaining thermoelectric ceramics with low electrical resistivities while being based on simple and reproducible processes.

4. Conclusions

Pure $Ca_3Co_4O_9$ phase powders were successfully prepared by environmentally friendly synthesis methods. The electrical characterization showed a performance optimization for the C349 ceramic obtained by the proteic sol-gel synthesis. Both proposed eco-friendly procedures showed competitive thermoelectric performance as compared to the literature data on C349 ceramics.

Conflict of interest

None.

Acknowledgements

This study was financed in part by the Coordenação de Aperfeiçoamento de Pessoal de Nível Superior - Brasil (CAPES) - Finance Code 001. Daniel A. Macedo acknowledges CNPq (Brazil, 311883/2016-8 and 431428/2018-2). The authors also acknowledge the support of FCT, Portugal with SFRH/BPD/124238/2016 grant, and UID/CTM/50011/2019 and POCI-01-0145-FEDER-031875 projects, financed by COMPETE 2020 Program and National Funds through the FCT/MEC and when applicable co-financed by FEDER under the PT2020 Partnership Agreement.

References

[1] A.I. Hochbaum, R. Chen, R.D. Delgado, W. Liang, E.C. Garnett, M. Najarian, A. Majumdar, P. Yang, Nat. Lett. 451 (2008) 163–167.

[2] M. Bittner, L. Helmich, F. Nietschke, B. Geppert, O. Oeckler, A. Feldhoff, J. Eur. Ceram. Soc. 37

(2017) 3909–3915.
[3] T.A. Tyson, Z. Chen, Q. Jie, Q. Li, J.J. Tu, Phys. Rev. B 79 (2009) 024109.
[4] M.A. Madre, F.M. Costa, N.M. Ferreira, A. Sotelo, M.A. Torres, G. Constantinescu, Sh. Rasekh, J.C. Diez, J. Eur. Ceram. Soc. 33 (2013) 1747–1754.
[5] N. Kanas, S.P. Singh, M. Rotan, M. Saleemi, M. Bittner, A. Feldhoff, T. Norby, K. Wiik, T. Grande, M.-A. Einarsrud, J. Eur. Ceram. Soc. 38 (2018) 1592–1599.
[6] S. Butt, Y.-C. Liu, J.-L. Lan, K. Shehzad, B. Zhan, Y. Lin, C.-W. Nan, J. Alloys Compd. 588 (2014) 277–283.
[7] S. Urata, R. Funahashi, T. Mihara, A. Kosuga, S. Sodeoka, T. Tanaka, Int. J. Appl. Ceram. Technol. 4 (2007) 535–540.
[8] M.G. Kang, K.H. Cho, J.S. Kim, S. Nahm, S.J. Yoon, C.Y. Kang, Acta Mater. 73 (2014) 251–258.
[9] F. Delorme, C.F. Martin, P. Marudhachalam, D.O. Ovono, G. Guzman, J. Alloys Compd. 509 (2011) 2311–2315.
[10] T. Schulz, T. Reimann, A. Bochmann, A. Vogel, B. Capraro, B. Mieller, S. Teichert, J. Töpfer, J. Eur. Ceram. Soc. 38 (2018) 1600–1607.
[11] G. Constantinescu, Sh. Rasekh, M.A. Torres, J.C. Diez, M.A. Madre, A. Sotelo, J. Alloys Compd. 577 (2013) 511–515.
[12] M. Presečnik, J. De Boor, S. Bernik, Ceram. Int. 42 (2016) 7315–7327.
[13] C. Boyle, P. Carvillo, Y. Chen, E.J. Barbero, D. Mcintyre, X. Song, J. Eur. Ceram. Soc. 36 (2016) 601–607.
[14] F. Kahraman, M.A. Madre, Sh. Rasekh, C. Salvador, P. Bosque, M.A. Torres, J.C. Diez, A. Sotelo, J. Eur. Ceram. Soc. 35 (2015) 3835–3841.
[15] A. Sotelo, Sh. Rasekh, M.A. Torres, P. Bosque, M.A. Madre, J.C. Diez, J. Solid State Chem. 221 (2015) 247–254.
[16] Z. Shi, J. Xu, J. Zhu, Y. Zhang, T. Gao, M. Qin, H. Sun, G. Dong, F. Gao, Ceram. Int. 45 (2019) 1977–1983.
[17] H. Fukutomi, Y. Konno, K. Okayasu, M. Hasegawa, H. Nakatsugawa, Mater. Sci. Eng. A 527 (2009) 61–64.
[18] A.I. Klyndyuk, I. V Matsukevich, Glas. Phys. Chem. 41 (2015) 545–550.
[19] R. Robert, S. Romer, A. Reller, A. Weidenkaff, Adv. Eng. Mater. 7 (2005) 303–308.
[20] E.B.G.A. Fulgêncio, F.J.A. Loureiro, K.P. V Melo, R.M. Silva, D.P. Fagg, L.F.A. Campos, D.A. Macedo, J. Alloys Compd. 788 (2019) 148–154.
[21] J.R.D. Santos, F.J.A. Loureiro, J.P.F. Grilo, V.D. Silva, T.A. Simões, D.P. Fagg, D.A. Macedo, Electrochim. Acta 285 (2018) 214–220.
[22] E.B.G.A. Fulgêncio, K.P.V. Melo, R.M. Silva, J.P.F. Grilo, V. Caignaert, M.R. Cesário, L.F.A. Campos, D.A. Macedo, Ceram. Int. 43 (2017) 9564–9567.
[23] Y.F. Zhang, J.X. Zhang, Q.M. Lu, Q.Y. Zhang, Mater. Lett. 60 (2006) 2443–2446.
[24] J.C. Diez, M.A. Torres, Sh. Rasekh, G. Constantinescu, M.A. Madre, A. Sotelo, Ceram. Int. 39 (2013) 6051–6056.
[25] D. Kenfaui, D. Chateigner, M. Gomina, J.G. Noudem, J. Alloys Compd. 490 (2010) 472–479.
[26] D. Kenfaui, G. Bonnefont, D. Chateigner, G. Fantozzi, M. Gomina, J.G. Noudem, Mater. Res. Bull. 45 (2010) 1240–1249.
[27] M. Mikami, S. Ohtsuka, M. Yoshimura, Y. Mori, T. Sasaki, R. Funahashi, M. Shikano, Jpn. J. Appl. Phys. 42 (2003) 3549–3551.
[28] J. Takahashi, H. Yamane, M. Shimada, Jpn. J. Appl. Phys. 43 (2004) L331–L333.

Figure
Click here to download high resolution image

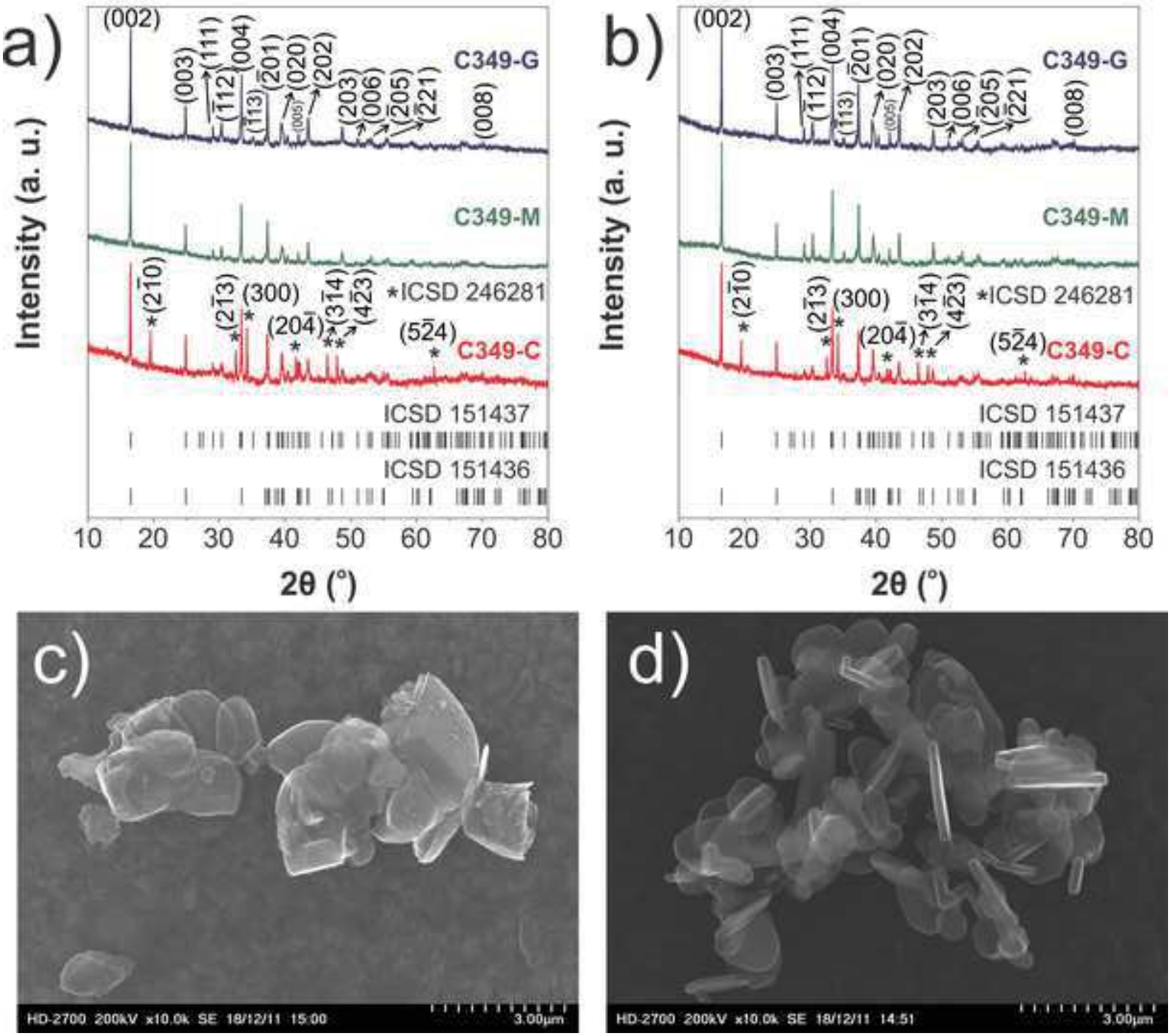

Figure
Click here to download high resolution image

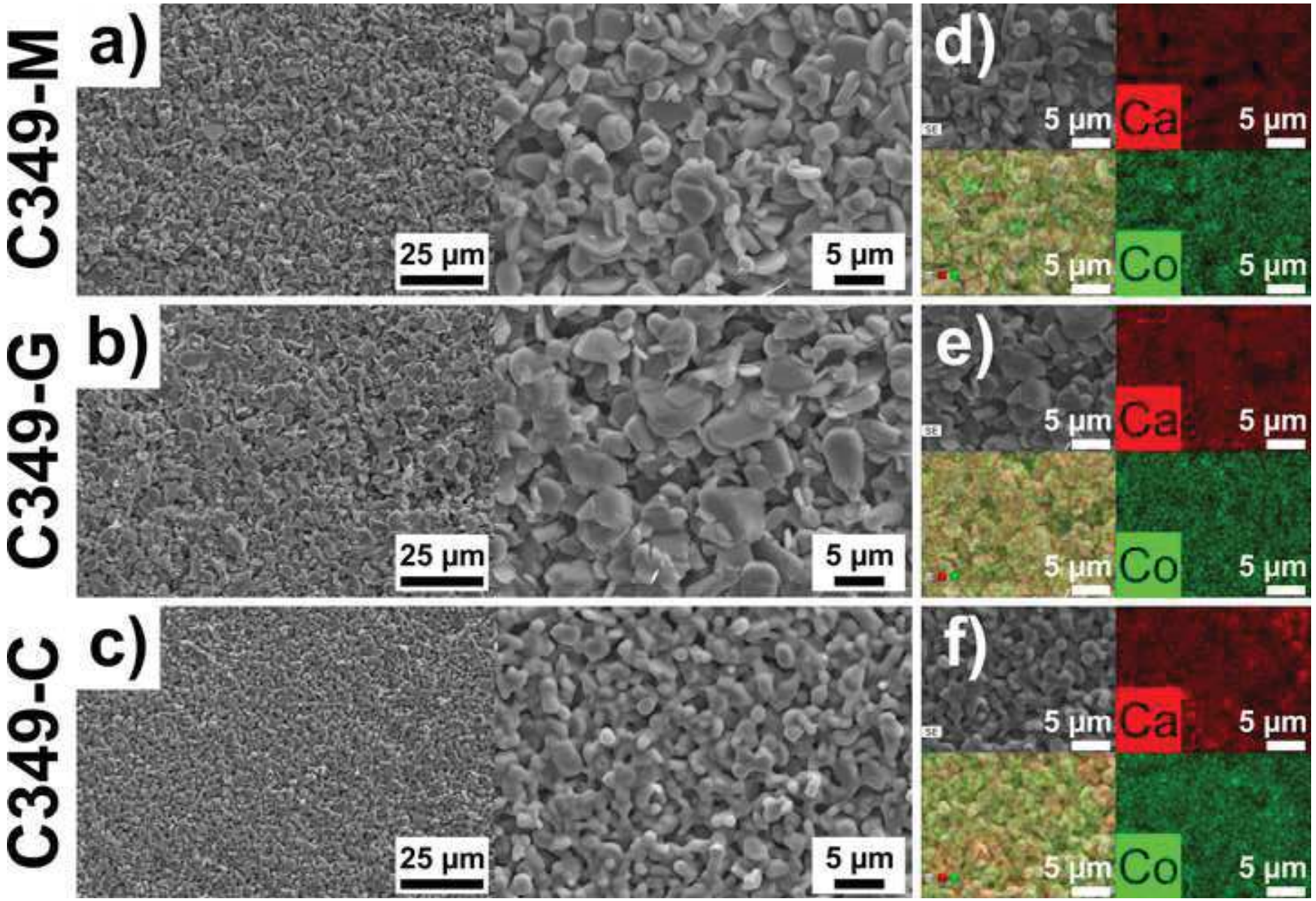

Figure
Click here to download high resolution image

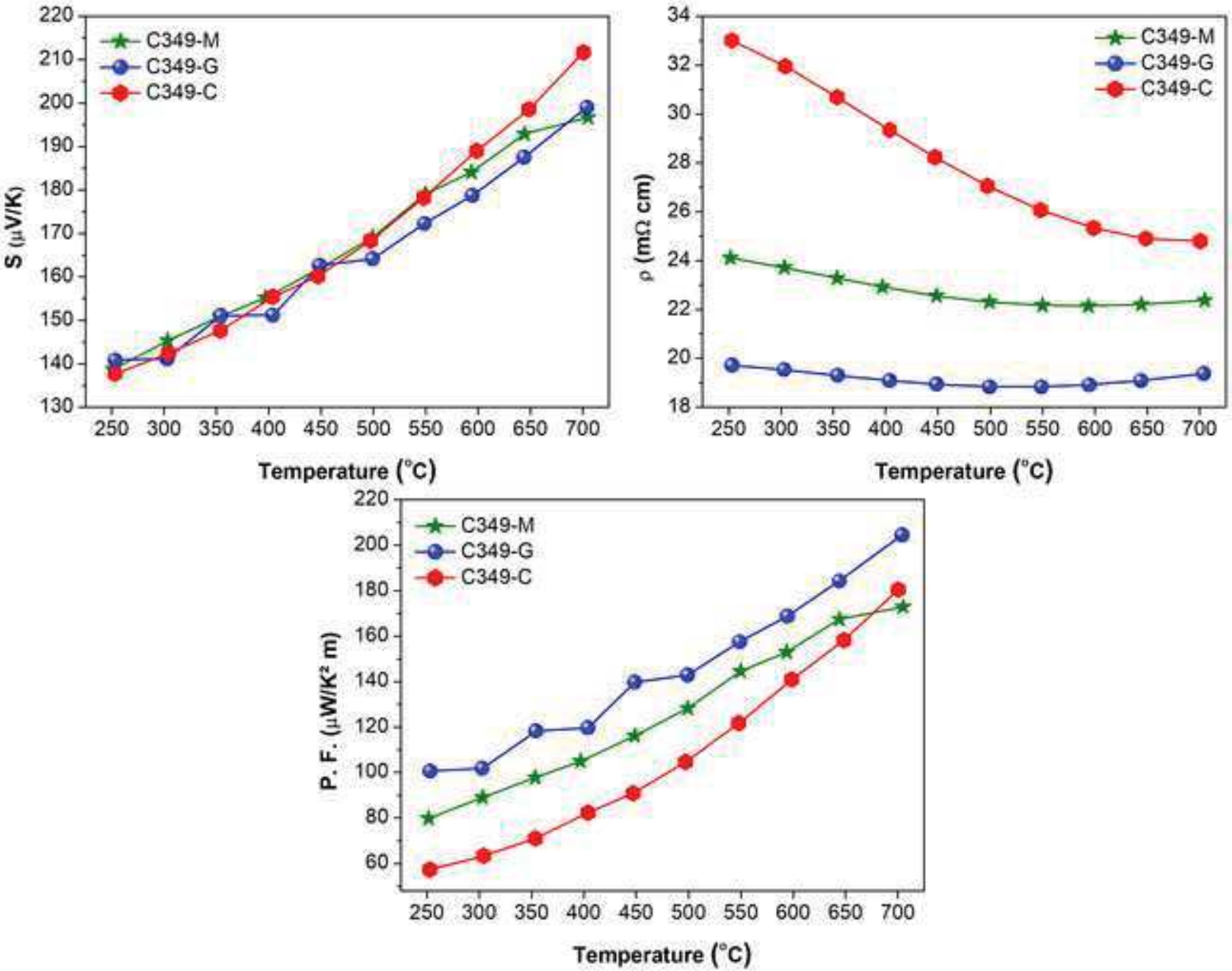

Electronic Supplementary Material (online publication only)

Click here to download Electronic Supplementary Material (online publication only): Supplementary data - C349 Eco-friendly syn